25. N. A. Dyatko, I. V. Kochetov, et al., "Effect of the ionization proess on kinetic coefficients in a low-temperature plasma," Preprint IAE No. 3842/12, Moscow (1983).
26. V. P. Silakov and A. V. Chebotarev, "Steady-state flow of an oscillating-excited gas of biatomic molecules," Prikl. Mekh. Tekh. Fiz., No. 5 (1986).

CONTRACTED DISCHARGE IN THE PRESENCE OF BOUNDARY LAYERS IN A SUPERSONIC PLASMA FLOW IN A CHANNEL

M. G. Musaev

UDC 537.533.5

This paper reports the results of an experimental study of the processes near the electrodes when a contracted discharge occurs in a pulsed supersonic channel. An analysis of the current-voltage characteristics and photoscans of the glow of the electrodes surfaces showed that in a pulsed supersonic argon plasma flow the resistance of the regions near the electrodes for divisible spots is lower than in the case of peripheral arc clamping. Then a decrease in the Mach number M_1 and the approach to a shock wave (in the zone of ionization relaxation) cause the current-voltage characteristics to shift to the right, i.e., to the region of a higher voltage drop between electrodes.

One of the simplest and most universal methods of studying the properties of an electric discharge in boundary layers is that of determining the current-voltage characteristics. When used in conjunction with a photoscan study of the discharge glow at the electrodes, depending on the state of the electrode surfaces and on the gasdynamic and thermophysical properties of the plasma in the channel, this method makes it possible to find more optimum operating conditions for the electrode walls of a pulsed cold-electrode MHD generator. The studies are complicated by the following: the existence of a boundary layer which moves relative to the electrodes and a longitudinal inhomogeneity of the initial portions of the gasdynamic plug because of ionization relaxation and the variation of the effective cross section of the gas flow behind the shock wave as boundary layers grow on the channel walls. The boundary layer can shorten the ionization relaxation to different degrees for laminar and turbulent layers [1, 2]. By the criteria of [2] the boundary layer is completely laminar provided that $p_1 d \leq 1.63 \cdot 10^3$ Pa·cm (d is the gasdynamic diameter of the tube and p_1 is the initial pressure in the chamber), while at $p_1 d \geq 16.3 \cdot 10^3$ Pa·cm the boundary layer becomes virtually turbulent along the entire length of the plug. In all other cases the nature of the boundary layer is determined only experimentally because of the lack of any theoretical model. The coordinates of the laminar-turbulent transition of the boundary layer depends on the critical Reynolds number [3]

$$\mathrm{Re}_{cr} = \rho \frac{(u_s - u_2)^2 X}{u_2 \mu_2},$$

where ρ, μ_2, and u_2 are the density, dynamic viscosity, and velocity of the flow in the coordinate system bound to the shock front, and u_s is the velocity of the shock-wave front in the laboratory coordinate system.

The time of the laminar-turbulent transition of the boundary layer is determined with a short-lag thermal resistance sensor, consisting of a thin metal film (platinum) deposited on a glass substrate [4].

Knowledge of the ionization relaxation zone makes it possible to isolate the region of shock-heated gas with an equilibrium electron concentration. The zone was calculated in the one-dimensional and quasi-one-dimensional (in the case of a turbulent boundary layer) approximations in the range of shock-wave Mach numbers M_1 = 8-12 over a wide range of p_1. The

Moscow. Translated from Prikladnaya Mekhanika i Tekhnicheskaya Fizika, No. 3, pp. 26-29, May-June, 1992. Original article submitted March 12, 1991.

0021-8944/92/3303-0331$12.50

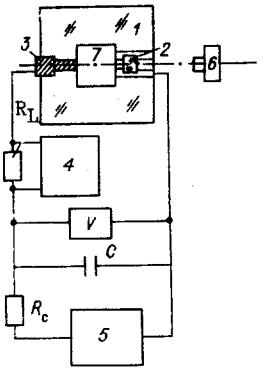

Fig. 1

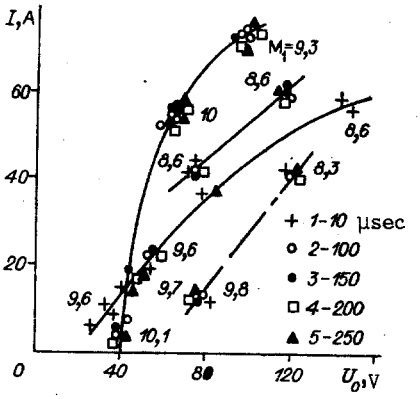

Fig. 2

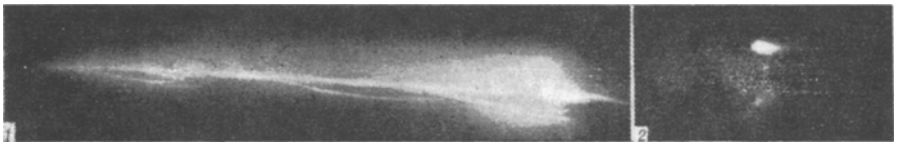

Fig. 3

ionization relaxation times were found from the variation of the intensity of the continuous argon radiation behind the shock wave [1] and the electrical conductivity σ. The basis for this was that in monoatomic gases primarily the electron concentration n_e varies behind the shock wave while the other parameters on which σ depends either change very little or remain virtually constant. For processing the conductivity sensor signals the distance from the front to the cross section in which the conductivity reaches 0.9 of its equilibrium value was chosen for the length X_{rel}. This choice was based on the result of a comparative analysis of the calculated profiles of the degree of ionization and the electrical conductivity in an argon shock wave.

The experimental study of the properties of shock-heated argon thus consisted of determining practical laminar-turbulent transition times of the boundary layer as well as the dimensions and structure of the nonequilibrium ionization-relaxation zone and electrical conductivity in the equilibrium zone.

The shock-wave Mach number $M_1 \approx 12$, the plasma equilibrium temperature was 10^4 K, the plasma velocity behind the shock wave was 3500 $m \cdot sec^{-1}$, the flow Mach number $M_2 = 1.6$, and the pressure behind the shock wave was about $2 \cdot 10^5$ Pa. The time taken by the zone of shock-compressed gas (gasdynamic plug) to pass through the measuring chamber placed in the region of the steady-state shock-wave velocity was ∿250 μsec.

We studied the phenomena near the electrodes in a pulse of the supersonic plasma flow behind the front of an incident shock wave in a shock tube by using a channel of constant cross section with a measuring dielectric section, containing two electrodes flush on the opposite walls of a section was a square cross section (7.2 × 7.2 cm), whose diagram is shown in Fig. 1, where 1 is a measuring chamber, 2 is T-shaped optical glass, 3 is a cathode, 4 is an oscilloscope, 5 is the charger of the capacitor bank C, 6 is a drum photorecorder, 7 is a hollow anode, V is a voltmeter, R_L is a load resistor, and R_c is a charging resistance. The experimental setup was described in greater detail in [5].

In studying the processes near the electrodes we recorded the current oscilloscope traces of pulse discharge of a capacitor bank with a total capacitance of $3 \cdot 10^3$ F at an initial voltage of 50-500 V across an electrode gap with a shock-compressed plasma and a series-connected load resistance ($R_L = 4$ Ω). During the passage of the gasdynamic plug the large capacitance of the capacitor bank ensures a virtually constant source voltage; this simplifies the processing of the current-voltage characteristic of the electrodes from the oscilloscope traces of the discharge current. An ultrafast drum photorecorder operating in the slave mode was used to record the photoscans of the discharge glow processes at the electrodes in the measuring section.

In Fig. 2 we show the current-voltage characteristics of the regimes of transient divisible and low-mobility cathode spots for various parameters of the shock-heated gas, obtained in a series of preliminary experiments. As the shock-wave Mach number M_1 and the plasma conductivity decrease, the characteristics for the divisible spots shift to the right, into the region of higher interelectrode resistance. The current-voltage characteristics far from the shock wave, deep in the gasdynamic plug, at $M_1 = 9.7$-10.1 have steep portions with rapidly growing current. The discharge current increases fivefold when the voltage changes by 10-15 V. At $\tau > 100$ μsec, i.e., in the equilibrium zone, the current-voltage characteristics do not significantly depend on the position of the shock wave relative to the electrodes for the same M_1 (τ is the discharge time after the electrodes are short-circuited with the arrival of the shock front). The bend in the current-voltage characteristic at $I > 50$ A may perhaps be a consequence of a lower plasma conductivity at $M_1 = 9.3$, which is consistent with the higher ohmic resistance of the interelectrode gap. Indeed, the plasma resistance is $R_{pl} = 1.1$ Ω at $M_1 = 10$ and $I = 50$ A and $R_{pl} = 1.5$ Ω at $M_1 = 9.3$ and $I = 7.3$ A.

Because of the low electrical conductivity at $M_1 = 9.3$-10 the current-voltage characteristics in the region of the relaxation zone also lie considerably to the right of those obtained for the regions of the plasma deep in the gasdynamic plug. A similar result was also obtained for $M_1 = 8.6$.

The intersection of the current-voltage characteristic of the relaxation zone with those obtained deep in the region of the shock-heated gas is attributed to the effect of the thickness of the thermal laminar boundary layer, which is smaller in the relaxation zone directly behind the shock wave than deep in the region of the shock-heated gas for points 2-5. Points 1 at $M_1 = 9.6$ and $I = 7.3$ and 10.1 A, therefore, lie above points 2-5. The differences in the discharge currents at $M_1 = 9.3$ for the time $\tau_1 = 10$ μsec as well as at $M_1 = 8.6$ are in agreement with the values of the conductivity in the relaxation and equilibrium zones [6].

A decrease in the Mach number M_1 and the approach to the shock wave with a corresponding decrease of the plasma conductivity shift the current-voltage characteristics to the right, to the region of a large voltage drop between the electrodes.

Figure 2 shows two groups of points, obtained in separate experiments, which fall outside the general laws. The points at $M_1 = 9.8$ ($U_{pl} = 80$ V) and 8.3 ($U_{pl} = 120$ V), according to high-speed photoscanning, correspond to a regime of peripheral immobile spots, while divisible spots were recorded at currents of about 45 A and interelectrode voltages of 70 V. Both divisible and immobile spots were observed at $M_1 = 8.6$ and $I \approx 60$ A [$U_{pl} = 110$ V) (Fig. 3) where 1 are photoscans of the glow of transient divisble cathode spots on a copper electrode, coated with an oxide film ($p_1 = 1.3 \cdot 10^3$ Pa, $U = 78$ V, $M_1 = 8.6$), 2 is the glow of nondivisible immobile cathode spots on a polished copper electrode ($p_1 = 1.3 \cdot 10^3$ Pa, $U = 80$ V, $M_1 = 9.8$)]. The transient divisible cathode spots encompass almost the entire surface of the electrode. The nondivisible spots are carried away by the flow and are deposited on the rear back edge of the electrode.

From the discussion above it follows that the resistance of the regions adjacent to the electrodes for divisible spots is lower than in the case of peripheral arc clamping, which is consistent with the data of [7], where the voltage drop became smaller as the number of spots on the elecrode increased.

In summary, the electrical characteristics of a discharge evidently are determined essentially by the form and position of the cathode spots: immobile cathode spots at the electrode edges have a higher ohmic resistance than do divisible transient spots.

LITERATURE CITED

1. E. V. Stupochenko, S. A. Losev, and A. I. Osipov, "Inhomogeneity of flow behind a shock front," in: Relaxation Processes in Shock Tubes [in Russian], Nauka, Moscow (1965).
2. G. Mairels, "Limitation of the operating time of a shock tube because of a turbulent layer on the wall," Raket. Tekh. Kosmonavtika, 2, No. 1 (1964).
3. Kh. A. Rakhmatulina and S. S. Semenova (eds.), Shock Tubes [Russian translation], Mir, Moscow (1962).
4. Yu. A. Polyakov, "Application of film sensors to the study of heat exchange in a dissociated gas flow," in: Physical Gasdynamics, Heat Exchange, and Thermodynamics of High-Temperature Gases [in Russian], Nauka, Moscow (1962).

5. M. G. Musaev, É. K. Chekalin, and L. V. Chernykh, "Properties of a contracted discharge in an inhomogeneous boundary layer at an electrode in a high-velocity plasma flow," Prikl. Mekh. Tekh. Fiz., No. 3 (1983).
6. V. A. Tishchenko, N. V. Khandurov, and É. K. Chekalin, "Study of ionization processes behind strong shock waves using a conductivity sensor," Zh. Tekh. Fiz., 14, No. 5 (1974).
7. A. V. Bogdans, V. A. Bashilov, V. M. Gribkov, et al., "Study of the regime of transient cathode spots on electrodes in the channel of an MHD generator," in: First Soviet–American Colloquium on MHD Energy Conversion [in Russian], Nauka, Moscow (1974).

OPTIMIZATION OF THE INTERNAL SOURCE IN THE PROBLEM OF MHD FLOW AROUND A SPHERE

V. I. Shatrov and V. I. Yakovlev

UDC 533.9

Studies on the effect of electromagnetic body forces on the hydrodynamic pattern of the flow around bodies propelled by internal sources of electromagnetic fields have become of interest in connection with the design of magnetohydrodynamic propellers for submarines and surface vessels (see, e.g., [1, 2] and their bibliographies). Such studies for the case of a sphere as an example were started in [3-5] for fixed sources, which were chosen from qualitative considerations and are not optimum.

Clearly, the distributions of the electric and magnetic potentials at the surface of the sphere should be optimum, ensuring that the electrical energy consumption for propulsion at a given speed be minimum. Our goal here is to formulate the complete variational problem for determining the optimum potentials, construct the solutions of some simplified (variational) problems, and analyze them.

1. We consider a sphere of radius a with an internal source of fields, which was described in [3]. Electromagnetic fields in a liquid are characterized by the scalar potentials

$$\mathbf{E} = -\nabla[\varphi(r, \theta)\sin m\alpha], \quad \mathbf{B} = -\nabla[\chi(r, \theta)\cos m\alpha]. \tag{1.1}$$

The velocity field is assumed to be axisymmetric,

$$\mathbf{v} = \frac{1}{r\sin\theta}\left(-\frac{1}{r}\frac{\partial\psi}{\partial\theta}\mathbf{e}_r + \frac{\partial\psi}{\partial r}\mathbf{e}_\theta\right), \tag{1.2}$$

and is described by the stream function $\psi(r, \theta)$ (the sense of the axisymmetry assumption and some considerations concerning its applicability are given in [3]). The functions $\varphi(r, \theta)$, $\chi(r, \theta)$, $\psi(r, \theta)$, and $w(r, \theta)$ [vorticity curl $\mathbf{v} = w(r, \theta)\mathbf{e}_\alpha$] are determined from the problem

$$L\varphi = \frac{m\chi}{r\sin\theta}w, \quad L\chi = 0 \tag{1.3}$$

$$\left(L = \frac{\partial^2}{\partial r^2} + \frac{2}{r}\frac{\partial}{\partial r} + \frac{1}{r^2}\frac{\partial^2}{\partial\theta^2} + \frac{1}{r^2}\frac{\cos\theta}{\sin\theta}\frac{\partial}{\partial\theta} - \frac{m^2}{r^2\sin^2\theta}\right);$$

$$-\frac{1}{2r}\left[\frac{\partial\psi}{\partial r}\frac{\partial}{\partial\theta}\frac{w}{r\sin\theta} - \frac{\partial\psi}{\partial\theta}\frac{\partial}{\partial r}\frac{w}{r\sin\theta}\right] + \frac{1}{\mathrm{Re}}\frac{1}{r\sin\theta}E^2(r\sin\theta w) + N\langle\mathrm{curl}_\alpha\mathbf{f}\rangle = 0; \tag{1.4}$$

$$E^2\psi - rw\sin\theta = 0 \quad \left(E^2 = \frac{\partial^2}{\partial r^2} + \frac{\sin\theta}{r^2}\frac{\partial}{\partial\theta}\frac{1}{\sin\theta}\frac{\partial}{\partial\theta}\right); \tag{1.5}$$

Novosibirsk. Translated from Prikladnaya Mekhanika i Tekhnicheskaya Fizika, No. 3, pp. 30-38, May-June, 1992. Original article submitted March 19, 1991.

0021-8944/92/3303-0334$12.50